

Received 12 July 2023, accepted 13 August 2023, date of publication 18 August 2023, date of current version 7 September 2023.

Digital Object Identifier 10.1109/ACCESS.2023.3306473

## RESEARCH ARTICLE

# Analysis of the Factors Influencing the Performance of Single- and Multi-Diode PV Solar Modules

DILIP YADAV<sup>1</sup>, NIDHI SINGH<sup>1</sup>, VIKAS SINGH BHADORIA<sup>2</sup>, VASILIKI VITA<sup>3</sup>,  
GEORGIOS FOTIS<sup>3</sup>, ELEFTHERIOS G. TSAMPASIS<sup>4</sup>, AND THEODOROS I. MARIS<sup>4</sup>

<sup>1</sup>Department of Electrical Engineering, School of Engineering, Gautam Buddha University, Greater Noida 201312, India

<sup>2</sup>Industry Integration Cell, Shri Vishwakarma Skill University, Palwal 121102, India

<sup>3</sup>Department of Electrical and Electronics Engineering Educators, School of Pedagogical and Technological Education (ASPETE), 14121 Heraklion, Greece

<sup>4</sup>Core Department, National and Kapodistrian University of Athens (NKUA), Psahna, Athens, 34400 Euboea, Greece

Corresponding author: Vikas Singh Bhadoria (vikasbhadoria@gmail.com)

This work was supported by the National and Kapodistrian University of Athens (NKUA).

**ABSTRACT** This paper presents a comparative analysis of single, double, and three-diode models for commercial and industrial photovoltaic (PV) cells. The efficiency of a PV system depends on various factors, including fill factor, material effect, temperature coefficient, interconnections, module degradation, solar irradiation, module temperature, soiling, potential induced degradation, PV module tilt angle, parasitic resistance, and shading effect. The results show that adding diodes decreases the maximum allowable power taken from a PV cell, resulting in the single-diode model with the highest efficiency of 99.9% at STC. As the temperature increases, the voltage decreases and the maximum power decreases to 4.044 watts/°C, while with the rise in irradiation, the maximum power value increases to 80.04 watts/100w/m<sup>2</sup>. A rise in temperature affects voltage and current values, while irradiation affects current values. An increase in series resistance decreases maximum power values by 216.785 watts/0.1-ohm, while shunt resistance increases maximum power by 0.0725 watts/100 ohm without significant change in current value.  $P_{max}$ ,  $V_{max}$ , and  $I_{max}$  values increase with a decrease in shading value. Two and three-diodes respond more effectively than single diodes at the lowest and maximum shading values. Total-Cross-Tied configurations perform more efficiently in various connections, while HC and BL connections have comparable I-V performance. However, BL and HC have low maximum power. MATLAB software is used for modeling and simulation, assisting researchers in understanding factors affecting solar PV system efficiency and diode models.

**INDEX TERMS** Diode model, interconnection, irradiation, shading, soiling, total cross-tied connections.

## I. INTRODUCTION

A typical definition of renewable energy source is energy derived from a resource swiftly replaced by a natural process, such as solar, wind power, biogas, etc. Renewable energy sources are environmentally friendly, inexhaustible, and cost-effective. Even after accounting for potential constraints, studies have repeatedly shown that renewable energy can provide a significant percentage of future electricity demand. PV energy is nowadays used in many applications in stand-alone systems [1], [2], grid-connected systems [3],

The associate editor coordinating the review of this manuscript and approving it for publication was Padmanabh Thakur .

Electric vehicles, storage systems, micro-grid [4], and hybrid systems to enhance the reliability of the power generation systems [5] by using alternative renewable energy like wind. When PV cells are exposed to solar energy, a PV cell/module/array generates electricity for running a PV system load. Earlier studies show that a PV model can be based on a single-diode model [6], [7], [8], a two-diode model [7], [8], and a three-diode model [8], [9]. According to the results and conclusion [7], [8], [9], the one /single diode model performs better than the two-diode model when determining the overall I-V characteristics. Mostly single-diode and two-diode models are used to study the output characteristic of the PV module as the increase in diodes decreases the maximum

TABLE 1. Research finding.

Reff.	Year	Work	Finding
[1],[2]	2021, 2022	Application in Standalone system.	The panel output can be increased using MPPT techniques and a boost converter.
[3],[4] and [5]	2022, 2022, 2023	Applications of PV module	Grid-connected systems, Electric vehicles, Storage systems, Micro-grid, and Hybrid systems
[6]	2020	Fast and Accurate Single-Diode model design	This article examines models to investigate the best fit for a PV solar module's I- V curve.
[7]	2020	Comparison of one- and two-diode model	The one-diode model outperforms the two-diode model concerning the estimation of the overall I-V characteristics.
[8]	2023	Modeling of Single diode model, double diode model, and triple diode model	A single diode has a better response than two and three-diode models.
[9]	2021	Performance analysis between single Two and three-diode model	The one-diode model provides accurate results related to the two-diode model for high-intensity solar irradiation.
[10]	2020	Single-diode model of five-parameter single-diode model	The I-V, and power-P-V characteristics of a photovoltaic module in different conditions.
[11]	2020	The cooling effect, dust effect with and without cooling, and coal effect with the Spray Cooling method	Cooling and cleaning of the panel increases the efficiency of the panel. Cooling with coal decreases efficiency.
[12]	2023	Cooling system for the photovoltaic panel using water	Front cooling provides a 9.64% enhancement in efficiency
[13],[14]	2017, 2019	This paper is a review study on factors affecting the efficiency and output of a PV system.	Given the review and study of factors affecting the PV performance like: High-temperature humidity, dust accumulation, and sea salt effect of Indonesia's tropical climate.

TABLE 1. (Continued.) Research finding.

			PV material, parasitic resistances, shading effects, dust, module orientation, weather conditions, geographical location, and cable thickness.
[15]	2017	Effect of temperature and irradiance on four commercial PV cells.	The maximum power decreases with values between 0.14% and 0.47% if the temperature increases by 1°C for the photovoltaic cells analysed.
[16], [17], [18]	2012, 2011, 2021	PV Array configurations under partial shaded conditions	TCT is the best configuration for symmetrical array sizes and HC configuration for asymmetrical array sizes.
[19]	2020	A survey was conducted to calculate PV degradation rates	First three years, the degradation rates are less than 0.6%, while in the next two years, the degradation rates almost increased by 40%.
[20]	2023	Performance of solar PV cells Temperature+ humidity + dust allocation	lowers power output by up to 60–70%.
[21]	2021	Effect of Different Radiation and Temperature	With the temperature rise, the voltage decreases, and temperature affects the current value.
[22]	2022	Influence of Shading on Solar Cell Parameters	Shading has a great impact on the solar panel, bypass diode is used in parallel to avoid the damage of cell/panel/model
[23]	2015	Improving the efficiency of PV by using the PCM technique.	A temperature increase of 1°C in silicon cells results in a 0.5% loss in efficiency. Adding a PCM layer to the PV module's backside or cooling its efficiency can be increased by 10%
[24]	2010	Potential Induced Degradation of solar cells and Panels	Anti-reflective coating and by reversing the switching polarity and high temperatures support regeneration can avoid the effect of PID.
[25]	2021	The optimum tilt angle of the solar collector and evaluation of the position	The surface area covered by the sun at 45° is 40% larger, and the intensity is 30% lower than at 90°

power and efficiency of the panel [9], [10]. It is important to note that numerous factors affect the efficiency of PV module when exposed to the outer environment, including fill factor, material effect, temperature coefficient, interconnections, degradation of PV module, variation in solar irradiation, module temperature, soiling, potential induced degradation, PV module tilt angle, parasitic resistance, and shading effect. Some of the research finding in terms of performance are illustrated below:

Water spraying with coal decreases efficiency [11]. Cooling can provide an average 9.64% enhancement in efficiency [12]. Maximum power decreases with values between 0.14% and 0.47% if the temperature increases by 1°C for the photovoltaic cells [13], [14]. The maximum power decreases with values between 0.14% and 0.47% if the temperature rises by 1°C for the photovoltaic cells [15]. Total-Cross-Tied (TCT) is the best configuration for symmetrical array size [16], [17], [18]. Degradation rates are less than 0.6% in the first three years, while in the next two years, the degradation rates almost increased by 40% [19]. Power output decreases by up to 60–70% [20], when temperature and humidity, are combined with dust allocation. With the increase in temperature, the  $V_{oc}$  value decreases fast, and the current has negligible change. In contrast, the increase in irradiation has more effect on the  $I_{sc}$  value of the panel [21]. Shading significantly impacts the solar panel by decreasing its overall performance. A bypass diode is used in parallel to avoid damage to the cell/panel/model [22]. Few researchers have given some solutions to improve the efficiency of the panel, by using the colling technique [11], cleaning the panels properly [11], allowing airflow gaps [12], changing the configuration of the panel [18], Avoid Shadows [22], adding a PCM layer [23], Anti-reflective coating [24], changing the optimal angle of the solar collector [25] and Schedule Preventive Checks these all solutions can increase the efficiency of the PV generation. Table 1 represents the finding of research done in this field of diode model and performance analysis.

A selection of diode models and factors affecting PV module performance is investigated in this research paper. The paper is organized as follows: Section II represents the equivalent circuit of different diode models that are based on the simple mathematical equations in terms of the photocurrent generated ( $I_{ph}$ ) by PV cells under illumination., the saturation current diode ( $I_0$ ), the reverse saturation current ( $I_{rs}$ ), and the current through shunt resistor ( $I_{sh}$ ). Section III gives a basic introduction and briefly explains the factors affecting PV performance. Section IV provides the simulation with and results of different modelled diode models. The I–V and P–V curves of the single, two, and three diode models are achieved and validated with a 901.2 W-PV panel to test the performance and to find out the efficient diode model at STC condition, with this the simulation results for the various parameters affecting the performance of the PV module are considered in the paper like, variation in solar irradiation, module temperature, parasitic resistance, and shading effect are discussed for single-diode, two-diode, and three-diode

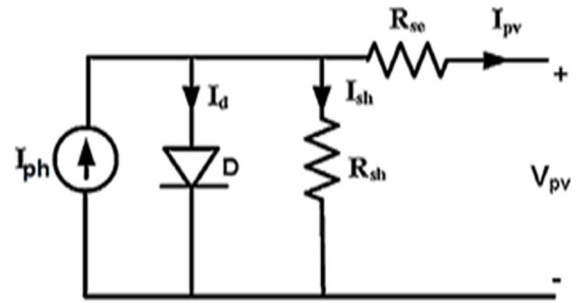


FIGURE 1. Basic PV cell circuit diagram.

models. Different interconnections are used to find the best interconnection among them. Section V presents the conclusion of the paper with its future implementation.

## II. PHOTOVOLTAIC MODEL

The PV cell modeling, which primarily associates the analysis of the efficiency curve and the non-linear current-voltage (I-V) and power-voltage (P-V) characteristics, is one of the most critical factors determining the PV system efficiency. According to [6], a current source connected in parallel with a diode is considered a basic equivalent model of a PV cell, as shown in Fig. 1. Previous studies by [7] show that the characteristics of the PV module and its efficiency are affected by non-linear environment conditions. Many mathematical models for modeling the performance of solar modules under various operating situations are discussed in [8], and different solar models are available in research studies [9].

As per [8], [9], and [10], single, double, and three-diode models can be used to model PV cells. In which photo electric current ( $I_{ph}$ ), diode current ( $I_d$ ), shunt resistance ( $R_{sh}$ ), series resistance ( $R_{se}$ ), and ideality factor ( $\eta$ ) are model parameters that will be used for calculating the PV current and voltage ( $I_{pv}$  and  $V_{pv}$ ).

### A. SINGLE DIODE MODEL

It is commonly known as the five-parameters model [10] and is mainly composed of series-parallel connected resistance and a diode, as depicted in Fig. 1.

$I_{pv}$  can be calculated by using the KCL, which is given as:

$$I_{ph} - I_d - I_{sh} - I_{pv} = 0 \quad (1)$$

$$I_{pv} = I_{ph} - I_d - I_{sh} \quad (2)$$

$$I_{sh} = \frac{V_{pv} + I_{pv} * R_{se}}{R_{sh}} \quad (3)$$

$$I_{rs} = \frac{I_{sc}}{\exp\left(q * \frac{V_{oc}}{n_s N_s * K * T}\right) - 1} \quad (4)$$

$$I_0 = I_{rs} \left(\frac{T}{T_n}\right)^3 * \exp\left[\frac{q * E_{go} * \left(\frac{1}{T_{ref}} - \frac{1}{T}\right)}{n_s * K}\right]$$

$$V_t = \frac{k * \eta * T}{q} \quad (5)$$

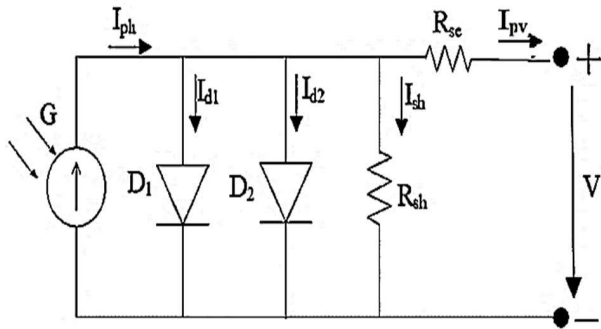


FIGURE 2. Two diode model.

$$I_{ph} = (I_{sc} + K \cdot (T - 298)) \cdot \left( \frac{G}{1000} \right) \quad (6)$$

Using Equation (2) to Equation (6),  $I_{pv}$  can be calculated as:

$$I_d = I_0 \cdot \left[ \exp \left( \frac{V_{pv} + I_{pv} R_{se}}{N_s \cdot V_t} \right) - 1 \right] \quad (7)$$

$$I_{pv} = I_{ph} - I_0 \cdot \left[ \exp \left( \frac{V_{pv} + I_{pv} R_{se}}{N_s \cdot V_t} \right) - 1 \right] I_{sh} \quad (8)$$

where  $I_{sh}$  is shunt current,  $K$  is the Boltzmann's constant equal to  $1.38 \times 10^{-23} \text{ J/K}$ ,  $q$  is the electron charge equal to  $1.602 \times 10^{-19} \text{ C}$ ,  $T$  is Temperature in kelvin,  $I_{pv}$  is the module output current,  $V_{pv}$  is the module output voltage,  $V_{oc}$  is open circuit voltage,  $I_{ph}$  is the photocurrent generated by PV cells under illumination,  $I_0$  is the saturation current of diod,  $I_{rs}$  is the reverse saturation current,  $I_{sh}$  is the current through a shunt resistor,  $I_{sc}$  is short circuit current,  $N_s$  is the number of cells, and  $V_t$  is the junction thermal voltage. As per [10],  $R_{se}$  is connected to account for the voltage drops and internal losses, were as  $R_{sh}$  is connected to account for the leakage current.

### B. TWO DIODE MODEL

The two-diode model is very similar to the single-diode model but includes a second diode parallel to the current source [7], [8], [9], as shown in Fig. 2.

$$I_{pv} = I_{ph} - I_{d1} - I_{d2} - I_{sh} \quad (9)$$

$$I_{pv} = I_{ph} - I_{01} \left( e^{\frac{V + I R_s}{n_{s1} V_t}} - 1 \right) - I_{02} \left( e^{\frac{V + I R_s}{n_{s2} V_t}} - 1 \right) - I_{sh} \quad (10)$$

where  $I_{d1}$  and  $I_{d2}$  are diode currents of diode  $D_1$  and  $D_2$ , in two diode model, two unknown ideality factors ( $\eta_{s1}$  and  $\eta_{s2}$ ) exist; therefore, the number of parameters increases which make it a little more complex than the single-diode model [8], but at lower temperature two diode model can withstand better, which act as an advantage [9].

### C. THREE DIODE MODEL

In the single and two-diode drops highlighted above, internal losses and voltage drops caused by the inflow of current in a PV cell are represented in the model by the series resistance [8]. The shunt resistance cares for the leakage current

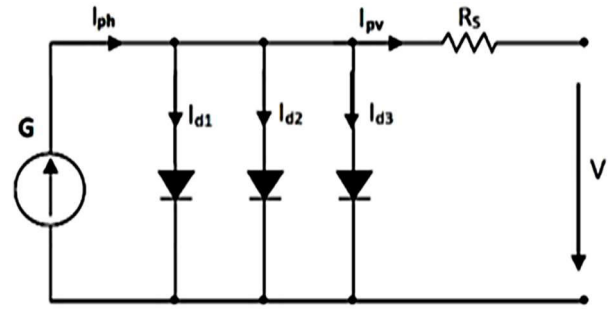


FIGURE 3. Three diode model.

to the ground in a practical PV cell. Fig. 3 represents the basic diagram of the three-diode model [9]. Using the concept of KCL.

$$I_{pv} = I_{ph} - I_{d1} - I_{d2} - I_{d3} - I_{sh} \quad (11)$$

$$I_{pv} = I_{ph} - I_{01} \left( e^{\frac{V + I R_s}{n_{s1} V_t}} - 1 \right) - I_{02} \left( e^{\frac{V + I R_s}{n_{s2} V_t}} - 1 \right) - I_{03} \left( e^{\frac{V + I R_s}{n_{s3} V_t}} - 1 \right) - I_{sh} \quad (12)$$

As per [2], [7], [11], [12], [13], [14] the accuracy of the model depends on the number of solar cells connected in a module, fill factor, and efficiency [11], [15].

$$\text{Fill Factor (F.F)} = \frac{V_m \cdot I_m}{V_{oc} \cdot I_{sc}} \quad (13)$$

$$\text{Efficiency } (\eta) = \frac{V_m \cdot I_m}{P_{in}} = \frac{V_{oc} \cdot I_{sc}}{P_{in}} \cdot F.F \quad (14)$$

$V_m$  is maximum power point voltage,  $I_m$  maximum power point current,  $V_{oc}$  is open circuit voltage,  $I_{sc}$  is short circuit current,  $P_{in}$  is input power (product of approximate irradiation and cell area), and F.F is filling factor. Equations (13) and (14) give the relationship between the fill factor and the efficiency of the PV module.

## III. FACTORS AFFECTING PV PERFORMANCE

The performance of a PV module depends on many factors which play an essential role in obtaining the desired output. The factors included in this paper are fill factor [11], cooling [12], temperature coefficient [13], [14], the material effect [15], parasitic resistance [13], [14], [20] different interconnections [16], [17], [18], degradation of PV module [19], soiling [11], [12], [13], [14], [20], a variation in solar irradiation [13], [14], [21], the shading effect [13], [14], [20], [22], module temperature [15], [20], [21], [23], potential induced degradation [13], [14], [24] and PV module tilt angle [25].

The effect of various factors of single and multi-diode models is given as follows: -

### A. FILL FACTOR

The fill factor (FF) is defined as the maximum power of the solar cell divided by the product of  $V_{oc}$  and  $I_{sc}$  as given in equation 14 [11]. According to [13], the fill factor is the area

**TABLE 2. The efficiency of Solar cell materials.**

Solar Cell Material	Efficiency	Temperature Coefficient (%/°C)
Polycrystalline	15-19%,	- 0.41
Monocrystalline	17-19.5%	-0.38
Polycrystalline PERC	17.5-18.5%,	-0.3 to -1
Monocrystalline PERC	17.5-19.8%,	-0.3 to -0.5
Monocrystalline N-type	19.8-20.7%	-0.35 to -0.41
Monocrystalline IBC	24.13%	-0.30
Heterojunction (HJC)	24%	-0.26

of the widest rectangle that fits in the I-V curve. A lower fill factor indicates a higher  $R_{se}$  or lower  $R_{sh}$  and lesser efficiency. A suitable PV module should have a fill factor above 70%. Low fill factors are generally caused by high series resistance [14].

### B. MATERIAL EFFECT

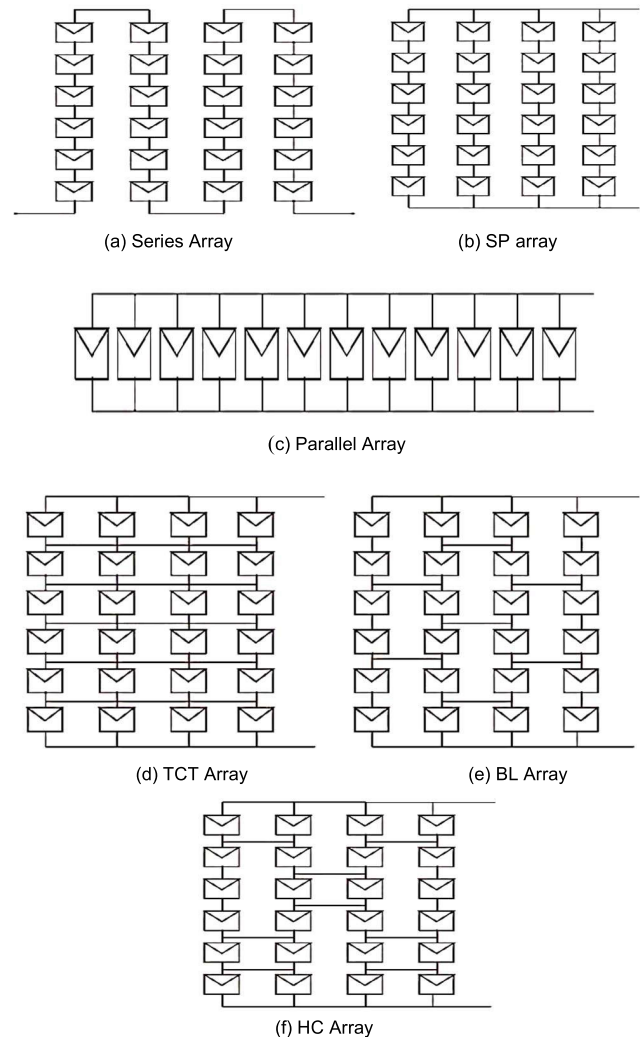
Previous studies [13], [14] show that currently, a wide choice of PV technologies is available in the market with efficiency and specifications, which helps the user to choose among them as per their need. Organic PV (OPV) and Concentrating PV (CPV) technologies are multi-junction and emerging technologies whose efficiency ranges from 15% to 16%. Passivated Emitter and Rear Cell (PERC) is a new technique that adds a dielectric passivation layer to the cell's rear to improve energy conversion efficiency. Back interdigitation (IBC) uses contact energy conversion instead of front contact. In PERC cells, the entire front of the cell can absorb sunlight, converting more photons to energy and improving the cells' efficiency. Based on the type of material used, the efficiency of the PV cell is given in Table 2 as per the manufactures data sheets available on the datasheet.

### C. TEMPERATURE COEFFICIENT

As per the previous study by [15], the power temperature coefficient (percent/°C) helps to choose the best manufacturer for efficiency and cost. The temperature coefficient of polycrystalline cells is -0.41 percent/°C, while monocrystalline cells have -0.38 percent/°C, monocrystalline IBC cells have -0.30 percent/°C, while HJC cells have -0.26 percent/°C as shown in Table 2 with few other. About 85% of the world's PV is crystalline silicon. Absolute temperature coefficients depend on the value of irradiance, and irradiance has little effect on open-circuit voltage but a lot on  $I_{sc}$  and  $P_{max}$ .

### D. INTERCONNECTION

The solar photovoltaic array configurations depicted in Fig. 4(a)-(f) are different interconnections of solar modules/panels having Series, Parallel, Series-Parallel (SP), Total Cross Tied (TCT), Bridge Linked (BL), and Honey-comb

**FIGURE 4. (a) Series, (b) SP array, (c) Parallel array, (d) TCT array, (e) BL array and (f) HC array configurations connections [16].**

(HC) [16]. The output voltage and current value can be changed using these different connections. According to [16], analysis of different connections using a physical solar photovoltaic module is not possible because field testing is expensive, time-intensive, and weather-dependent, so in most cases, the software is used for analysis purposes [17]. Previous research [16], [17] concluded that the TCT configuration outperforms better than the other five setups, but the interconnections with results were not kept constant for all. As per [18] TCT is the best configuration for symmetrical array sizes and HC configuration for asymmetrical array sizes.

### E. DEGRADATION OF PV MODULE

Solar PV manufacturers generally guarantee a 25-year module performance life. As shown in Fig. 5, the warranty curve guarantees 10% degradation in the first ten years and around 20% in the next 10-15 years. Variable losses and temperature effects contribute to overall PV deterioration loss.



FIGURE 5. The lifespan graph of typical solar PV modules [14].

Reference [19] compared the manufacturer values to the observed and found a 0.3 percent acceptable error. As per [13], CdTe and CIGS thin-film PV modules deteriorate more quickly than conventional Si PV modules. Chemical, electrical, thermal, or mechanical degradation mechanisms exist in PV modules. Inadequate design, materials, or production can cause early PV module deterioration.

F. VARIATION IN SOLAR RADIATION

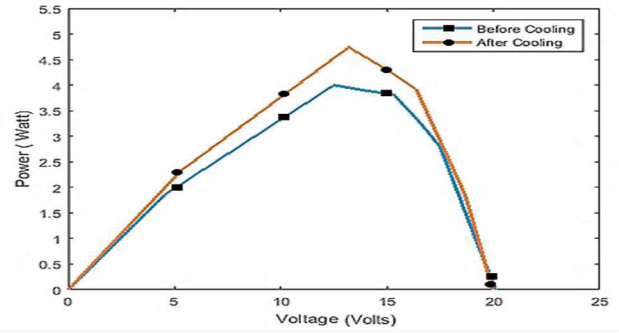
PV module performance varies significantly under different irradiance conditions, affecting PV system yield. Several parameters of a PV module are affected by variations in solar radiation intensity in terms of  $I_{max}$  and  $V_{max}$ . The rise in solar radiation raises the output current until the cell’s temperature interferes and lowers it. According to [19], [20], and [21], the rise in cell temperature has a more significant influence on the voltages than the rise in current.

G. MODULE TEMPERATURE

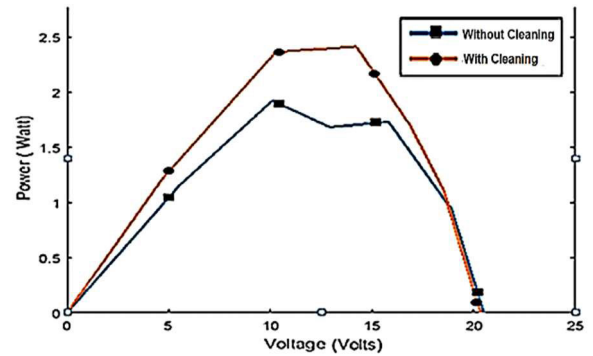
An increase in solar radiation and atmosphere temperature raises the PV module’s temperature, whereas a decrease in wind speed decreases temperature. Increased temperature causes a minor rise in cell current, but the voltage decreases faster, resulting in a more significant decrease in power output (from normalized values at 25°C). As per [19], [20], [21], and [22], if the cell’s temperature varies from the standard value of 25°C, the current increases and decreases, which changes the module’s power. According to [23], a temperature increase of 1°C in silicon cells results in a 0.5% loss in efficiency. Adding a PCM layer to the PV module’s backside or cooling its efficiency can be increased by 10% [23]. As per [11] before cooling the efficiency was 15.72% and after cooling the efficiency improved to 18%. Fig.6 (a) gives the effect of cooling on a module showing without and with cooling.

H. SOILING

Dust, sand, and other pollutants can damage a PV module. Particles smaller than 500 microns make up dust. According to [14], PV system soiling might result in a 5-17 % annual power loss. Soiling is a crucial reason for the O&M costs of PV plants. Cleaning should be done correctly to keep the module’s performance high. References [11] and [20] shows that cleaning enhances the power output. After the dust accumulation the efficiency was recorded as 3.363% and



(a) PV curve before and after cooling



(b) Effect of dust with and without cleaning [11].

FIGURE 6. P-V curve (a) before and after cooling, (b) effect of dust with and without cleaning [11].

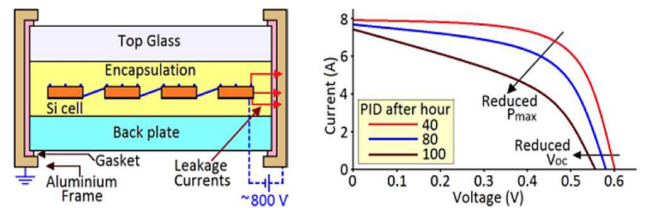


FIGURE 7. Paths of leakage currents during PID [14].

after cleaning the efficiency improved to 4.14%, as s shown in Fig. 6 (b) [11].

Dust, humidity, and soiling greatly influence PV system performance, it lowers power output up to 30-70% [20].

I. POTENTIAL INDUCED DEGRADATION

When stray currents induce a gradual loss of power up to 30%, this is known as Potential Induced Degradation (PID) [24]. PID mainly occurs due to surface functionalization, which promotes recombination and damage to the cell.

PID appears just a few years after a PV system is installed. The potential differences between some end-string modules and the module frame are significant. According to Fig. 7, certain electrons from PV cells can escape and discharge via the grounded frame [14]; PID also reduces the  $P_{max}$  and  $V_{oc}$  of a PV module. PID becomes more noticeable at higher temperatures, and the  $I_{sc}$  drop increases with PID. It can be minimized or controlled by using an

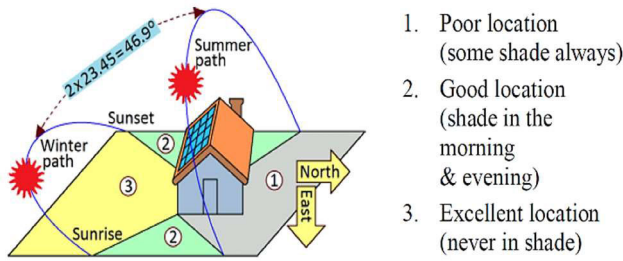


FIGURE 8. Shades are caused by a PV system’s orientation [14].

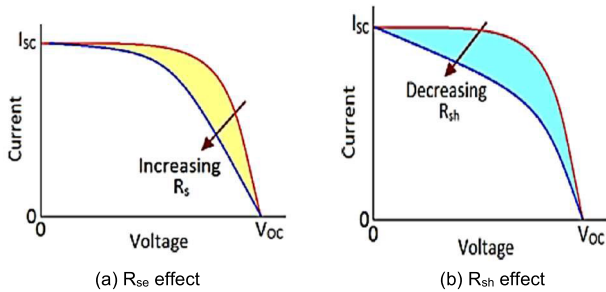


FIGURE 9. (a) Series resistance ( $R_{se}$ ), (b) Shunt resistance ( $R_{sh}$ ) effect on the I-V curve [14].

anti-reflective coating to avoid the effect of PID. Switching the polarity and high temperatures to support regeneration can reduce PID [22].

J. PV MODULE TILT ANGLE

PV modules have to face the true South, not the Northern Hemisphere’s magnetic South. As illustrated in Fig. 8, the intensity and duration of sunlight will change substantially in different directions due to shading. According to [25], the surface area covered by the sun at  $45^\circ$  is 40% larger, and the intensity is 30% lower than at  $90^\circ$ .

Depending on the region, optimal tilt angles range from  $1^\circ$  to  $67^\circ$ . Calculating the optimal tilt angle is possible. Optimal angles for systems with high solar fraction vary from  $\Phi$  (optimal tilt angles) to  $\Phi + 20^\circ$ .

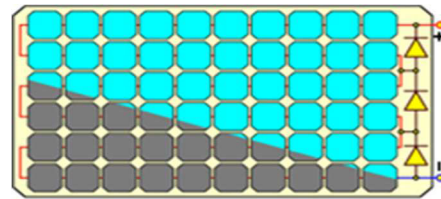
K. PARASITIC RESISTANCE

The shunt resistance ( $R_{sh}$ ) is responsible for the leakage current.  $R_{se}$  is the parasitic resistance. Resistances increase heat losses ( $I^2R$  losses) and reduce PV cell efficiency. Fig. 9 represents the effect of series and shunt resistance on the I-V curve, which shows that the reduction of area under the curve reduces fill-factor; hence, cell efficiency is also affected. According to [13] and [14], a PV module’s performance is optimized when  $R_{se}$  is low, and  $R_{sh}$  is high. These resistance values are essential for evaluating a PV system’s quality and performance.

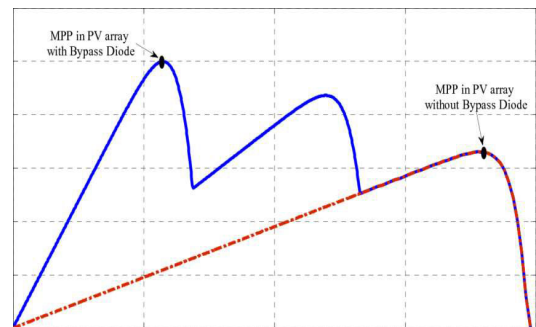
PV module data sheets usually do not include  $R_{se}$  and  $R_{sh}$ , although they may be computed. Table 3 displays the estimated  $R_{se}$  and  $R_{sh}$  for limited NTPC PV modules.

TABLE 3.  $R_{sh}$  and  $R_{se}$  of PV Cells for NTPC [14].

Location with a power rating	$R_{se}/\text{cell}$ (ohm)	$R_{sh}/\text{cell}$ (ohm)
Power Management Institute (295) Watt	4.529	7.181
Port Blair (235) Watt	3.674	6.610
Dadri (240) Watt	3.535	7.017
Faridabad (230) Watt	3.818	7.383
Singrauli (240) Watt	3.543	7.15



(a) Arrangement of a bi-pass diode



(b) Shading effect on I-V and P-V curve

FIGURE 10. (a) Arrangement of a bi-pass diode (b) Shading effect on I-V and P-V curve.

L. SHADING EFFECT

Trees, clouds, nearby buildings, or other things can shadow certain modules in a PV array. Shaded cells produce less current than un-shaded cells. A shaded cell that receives more current than it can handle may get overheated and perhaps damaged. There should be a gap between the PV modules determined depending on location and module size to avoid shading. According to [22], bypass diodes are a typical way to eliminate shading-induced PV cell hotspots.

The results revealed that 44 % shadowing of the first PV cells reduced the output power by almost 80%. Fig. 10 (a) shows a PV module having sixty cells with three bypass diodes, and Fig. 10 (b) represents the I-V and P-V curves during partial shade circumstances for polycrystalline PV modules operation.

IV. SIMULATION AND RESULTS

As discussed in section II, a single, two, and three-diode model consists of five unknown parameters, i.e.,  $I_{pv}$ ,  $R_{sh}$ ,  $R_{se}$ ,  $I_{ph}$ , and  $\eta$ , which are utilized for designing the PV

TABLE 4. Configuration of diode model.

Parameters	Symbol	Values
Short circuit current of a cell at 25°C and 1000 W/m <sup>2</sup>	$k_i$	0.0032
Open circuit voltage module (V)	$V_{oc}$	36.3
Short circuit current module (A)	$I_{sc}$	7.84
Electron charge (C)	$q$	$1.6 \times 10^{-19}$
Boltzmann's constant (J/K)	$K$	$1.389 \times 10^{-23}$
Ideality factor	$\eta$	1.3
Band gap energy (eV)	$E_{go}$	1.1
Shunt resistance ( $\Omega$ )	$R_{sh}$	313.399
Series resistance ( $\Omega$ )	$R_{se}$	0.3938
Operating temperature (K)	$T_{ref}$	25
Nominal temperature (K)	$T_n$	298
Solar Irradiation (W/m <sup>2</sup> )	$G$	1000
Number of cells in series	$N_s$	60
Open circuit voltage panel	$V_{oc}$	72.6
Short circuit current panel	$I_{oc}$	15.68
Maximum Voltage Panel	$V_{mp}$	60
Maximum current panel	$I_{mp}$	15.02

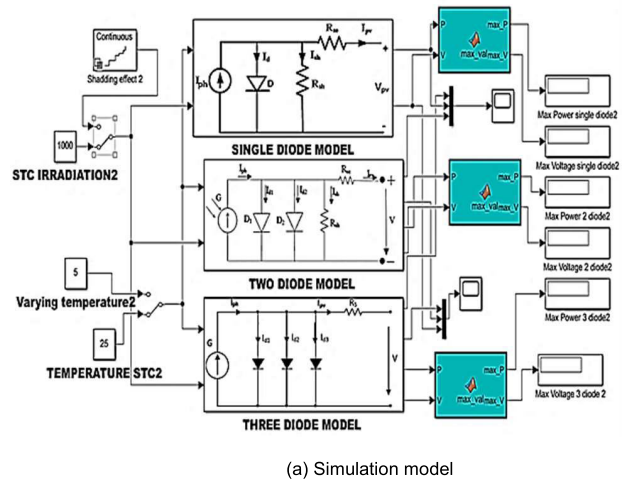
model. PV equations from (1)-(12) are used for modeling the single, double, and three-diode models. Input variables for the panel are irradiation, temperature, and output in terms of the current, voltage, and power, which define the performance of the PV panel in terms of its efficiency. The output of the different diode models are in term of  $I_{pv}$  represented by Equation (8) that, which is the combination of Equation (3), Equation (4), Equation (5), and Equation (6) that is in terms of  $I_{sh}$  (shunt resistor current),  $I_{rs}$  (reverse saturation current),  $I_o$  (saturation current) and  $I_{ph}$  (photocurrent generated these all mathematical Equations are modelled in the simulation software to get the final output of the panel in terms of  $I_{pv}$  (7) represents the output of the single diode current ( $I_d$ ).

In the case of two diode models, the diode current ( $I_d$ ) values get split into two diode currents ( $I_{d1}$  and  $I_{d2}$ ), as given in Equation (10). In the three-diodes model, the output current is divided into three diode currents ( $I_{d1}$ ,  $I_{d2}$ , and  $I_{d3}$ ), as given in Equation (12). By transforming the mathematical equations, i.e., Equation (7, 10, and 12), a simulation model is designed as shown in Fig. 11(a), representing the complete diode model of single, double, and three diode models. The designed sub-system of the PV panel is illustrated in Fig 11(b), showing the main equations of PV design.

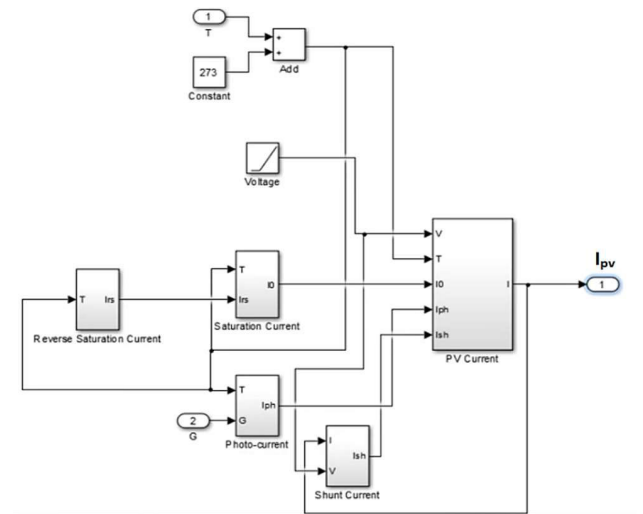
A. I-V AND P-V CURVES AT STC FOR SINGLE, DOUBLE, AND THREE-DIODE MODELS

A single diode model is designed by considering the cell parameters given in Table 4 and equations (1)-(8). By considering equations (9)-(10), two diode model is designed, and considering equations (11)-(12), three diode model is designed. PV module is designed for a single module of 60 cells with two series and two parallel modules with a maximum output power of the 901.2-Watt system.

A complete Simulink model and the result of the diode models are given in Fig. 11. P-V and I-V characteristics of the



(a) Simulation model

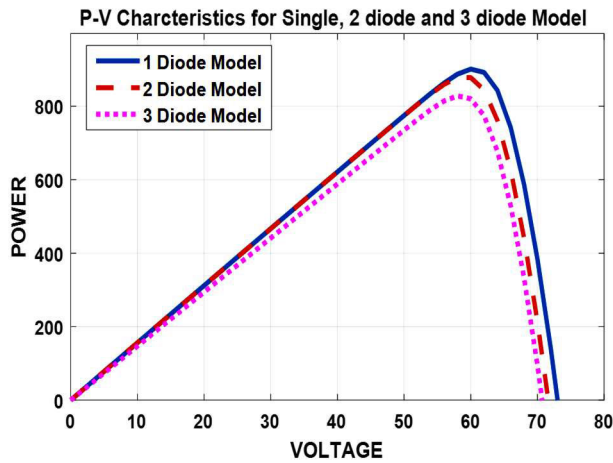


(b) Sub-System of PV panel

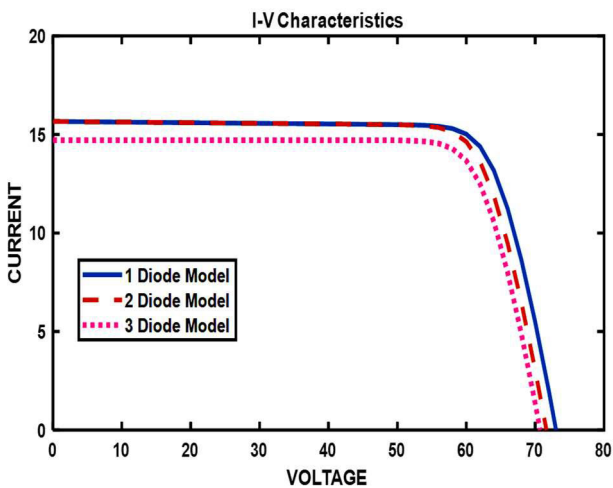
FIGURE 11. (a) Simulation model of Single, Double, and Three diode models. (b) Sub-System of the PV panel includes  $I_{sh}$ ,  $I_{rs}$ ,  $I_o$ ,  $I_{ph}$ , and  $I_{pv}$ .

single, two, and three-diode models are given in Fig. 12 (a) and Fig. 12 (b). The single-diode model has a maximum current ( $I_{max}$ ) of 15.01 Amp, maximum voltage ( $V_{max}$ ) of 60 volts, and maximum power ( $P_{max}$ ) of 901.1 watts, while the two and three-diode models have  $P_{max}$  of 878 watts and 847.5 watts, respectively. As per the specification, the maximum power a panel can withstand is 901.2 watts. The single-diode model has attained the maximum power of 901.1 watts, and the minimum error can be found between the actual value (as per MATLAB) and the designed model. Table 5 shows the outcome from the simulation of the diode models in terms of maximum voltage ( $V_{max}$ ), current ( $I_{max}$ ), and Power ( $P_{max}$ ). The P-V and I-V curves clearly show that the single-diode variant performs better at STC.

The  $P_{max}$  of the three-diode model is lower than other variants. The results show that adding diodes decreases the maximum allowable power taken from a PV cell. At STC, the efficiency of the single-diode model is 99.9%, two diode



(a) P-V characteristics



(b) I-V characteristics

**FIGURE 12.** (a) P-V characteristics, (b) I-V characteristics of single, double, and three diode model models at STC.

model is 97.4%, and three diode model is 94.04%, which proves that the performance of the single-diode model is much better than the two and three-diode models.

A model is built to assess the influence of factors on the P-V and I-V curves of solar modules (Table 4). Fig. 11 shows simulation models of three diodes, two diodes, and a single diode constructed in MATLAB 2020a version. Simulation results are obtained by changing only one parameter at a time to analyze the effect of other parameters while the other parameters are kept constant.

### B. EFFECT OF TEMPERATURE

Fig. 13 (a), (b), and (c) represents the I-V and P-V characteristics of single-diode, two-diode, and three-diode models at different temperature. Table 6 gives the voltage, current, and power values at different temperatures 5°C, 15°C, 25°C, 35°C, and 50°C. From Fig. 13 and Table 6, it can be concluded that with the rise in the value of temperature from 5°C to 50°C, the  $V_{max}$  values decrease at a fast rate, i.e., from

**TABLE 5.** Simulation result for different diode models.

Model	$P_{max}$ (watt)	$V_{max}$ (Volts)	$I_{max}$ (Ampere)
Single Diode	901.1	60	15.01
Two Diode	878	60	14.63
Three Diode	847.5	58	14.60

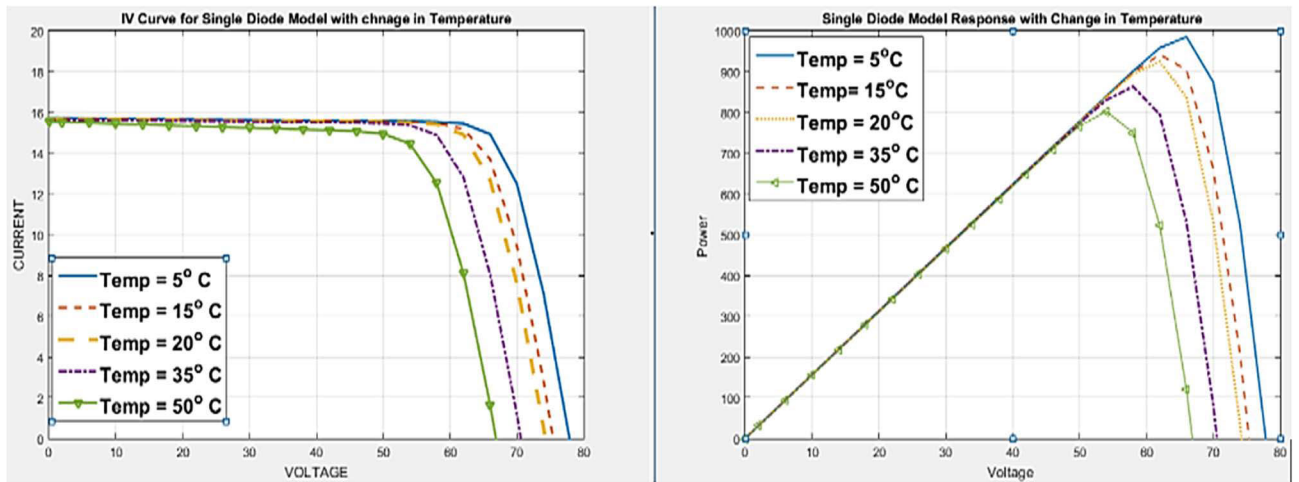
66-54 volts, which means there is a decrease of 0.266 volt/°C in maximum voltage value, whereas a small change can be seen in the maximum current value, i.e., decrement of 0.0164 amp/°C (15.02-14.82 amp) and high variation in the maximum power value, i.e., decrement of 4.044watts/°C (982-800 watts) with the increase in the temperature. From this analysis, it can be concluded that maximum voltage decreases as temperature increases, and minimal fluctuation occurs in the maximum current value.

### C. EFFECT OF IRRADIATION

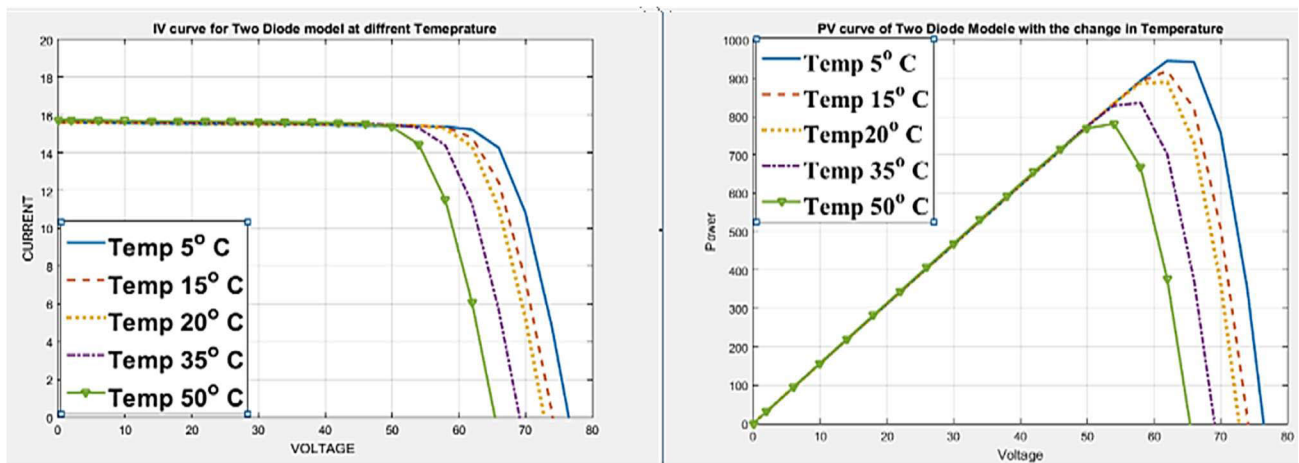
I-V and P-V curve obtained from the simulation models is shown in Fig. 14 (a), (b), and (c). It illustrates the irradiation effect on the single, two, and three-diode models at 100, 300, 500, 800, and 1000 w/m<sup>2</sup> irradiation values. Table 7 compares different irradiation values of single, two, and three-diode models. Table 7 shows that the single-diode model performs best in terms of  $P_{max}$ ,  $V_{max}$ , and  $I_{max}$ . As per Table 7 and Fig. 14, it is found that among single, two, and three-diode models, the maximum power is attained by the single-diode model at all irradiation values (100-1000w/m<sup>2</sup>), and from the analysis, it can be concluded that with the increase in the value of irradiation from 100-1000w/m<sup>2</sup> there is an increase in the Maximum power value of 80.04 watts with per 100w/m<sup>2</sup> rise in irradiation value. The current value increases at 0.1367 amp/100 w/m<sup>2</sup> value. There is very little change in the maximum voltage value with the rise in the irradiation value (60-62 volts), i.e., 0.02 volts/ 100w/m<sup>2</sup> irradiation value. From the analysis point of view, it can be concluded that irradiation has less impact on the maximum voltage. In contrast, irradiation has a high impact on current and power value. With the increases in irradiation, current and power value increases at a higher rate. The single-diode model has a better response than the two and three-diode models.

### D. EFFECT OF SERIES RESISTANCE ( $R_{se}$ )

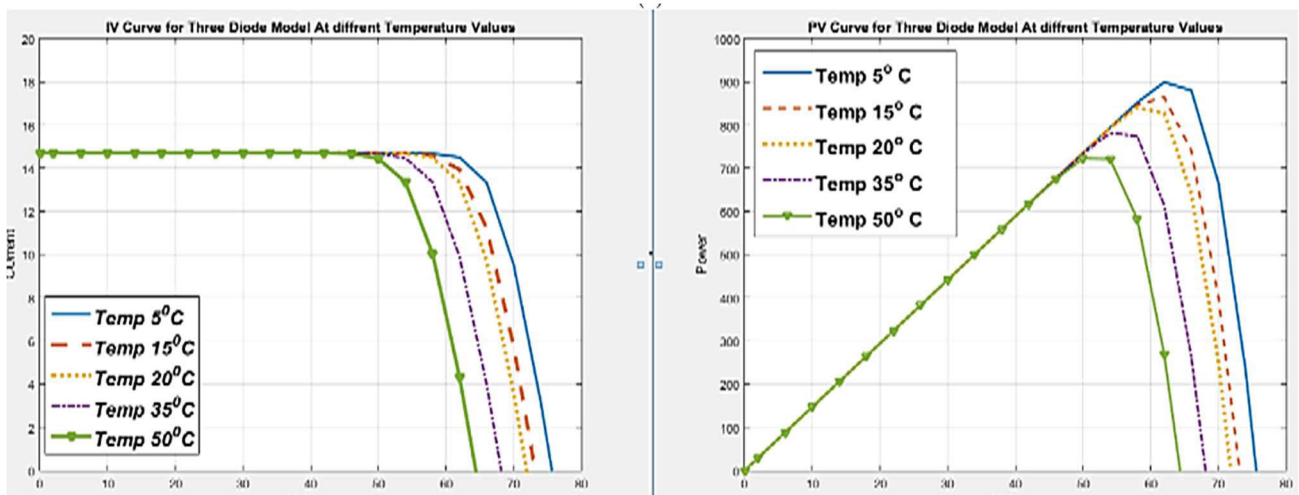
The voltage drops increase with current as the series resistance between the terminal and junction voltage increases. Fig. 15 (a-c) shows the influence of  $R_{se}$  on I-V and P-V curves at STC. All models' output power decreases as  $R_{se}$  increases. Variation in  $R_{se}$  is taken as 0.1, 0.3, 0.5, 0.9, and 1.5 ohms at STC condition, and  $R_{sh}$  is 313.399 ohm which is kept constant. It can be observed from Table 8 and Fig. 15 that with the increase in the series resistance value from 0.1 to 1.5 ohm, the value of maximum voltage decreases from 64-46 volts, i.e., with the rise of 0.1 ohms in the series resistance value every time there is a decrease of 12.85714 volts in the maximum voltage value of single diode model. In contrast,



(a) Single Diode Model



(b) Two Diode Model



(c) Three Diode Model

FIGURE 13. (a) Single diode (b) Two Diode model (c) Three diode I-V and P-V characteristics at different temperatures.

**TABLE 6. Effect of temperature on PV module.**

Temp. (°C)	Single Diode			Two Diode			Three Diode		
	$P_{max}$	$V_{max}$	$I_{max}$	$P_{max}$	$V_{max}$	$I_{max}$	$P_{max}$	$V_{max}$	$I_{max}$
5	982	66	15.02	956.6	64	14.94	905.4	64	14.94
15	940.1	62	14.86	918.4	62	14.8	864.3	62	14.8
20	921.6	62	15.15	899.6	60	14.99	847.8	60	14.99
25	901.1	60	14.87	878	60	14.63	847.5	60	14.63
35	861	58	14.84	842.1	56	15.04	790	56	15.04
50	800	54	14.82	784.1	52	15.08	732.6	52	15.08

**TABLE 7. Effect of irradiation on PV models.**

Irradiation w/m <sup>2</sup>	Single Diode			Two Diode			Three Diode		
	$P_{max}$	$V_{max}$	$I_{max}$	$P_{max}$	$V_{max}$	$I_{max}$	$P_{max}$	$V_{max}$	$I_{max}$
100	80.61	60	1.34	78.76	60	1.13	34.01	58	0.58
300	269.6	60	4.349	263.6	60	4.394	216.2	60	3.603
500	456.3	62	7.36	446	60	7.43	397.1	60	6.61
800	725.1	62	11.7	711.1	60	11.85	657.9	60	10.97
1000	901	60	15.01	878	60	14.63	847.5	58	14.60

**TABLE 8. Effect of series resistance on I-V and P-V curves.**

Model	$R_{se} = 0.1 \text{ ohm}$			$R_{se} = 0.3 \text{ ohm}$			$R_{se} = 0.5 \text{ ohm}$			$R_{se} = 0.9 \text{ ohm}$			$R_{se} = 1.5 \text{ ohm}$		
	$P_{max}$	$V_{max}$	$I_{max}$												
Single	966.5	64	15.1	901	60	15.6	875.5	58	15.09	789.9	54	14.63	663	46	14.41
Two	899.1	60	14.98	878	60	15.58	866.7	58	14.94	789	54	14.61	663	46	14.41
Three	836.7	60	13.94	847.5	58	14.71	819.5	58	14.13	756.7	54	14.01	641.5	48	13.36

$R_{se}$  affects both voltage and current values, and there is a decrease in power for all models.

**TABLE 9. Effect of shunt resistance on I-V and P-V curves.**

Model	$R_{sh} = 100 \text{ ohm}$			$R_{sh} = 200 \text{ ohm}$			$R_{sh} = 313.3 \text{ ohm}$			$R_{sh} = 500 \text{ ohm}$		
	$P_{max}$	$V_{max}$	$I_{max}$	$P_{max}$	$V_{max}$	$I_{max}$	$P_{max}$	$V_{max}$	$I_{max}$	$P_{max}$	$V_{max}$	$I_{max}$
Single	876.4	60	14.61	894.5	60	14.911	901.1	60	15.6	905.4	60	15.09
Two	854.8	60	14.25	871.8	60	14.53	878	60	15.58	882	60	14.7
Three	716.5	58	12.35	798.6	58	13.77	847.5	58	14.71	847.3	58	14.61

With the increase in the value of  $R_{sh}$ , Power increases.

the two-diode model has a decrement of 27.14 volts, and the three diodes have 25.714 volts. From 0.3 to 1.5-ohm value, the single-diode and two-diode models have the same maximum voltage value. Initially, from 0.1-0.5 ohm, the maximum current values have a slight increase in the value, i.e., 15.1-15.6 amp, and after that, its value decreases from 15.6-14.41 amp for 0.3-1.5-ohm value.

The single-diode model attains the maximum power with respect to the two and three-diode models, and the maximum power decreases at a value of 216.785 watts with the increase

of 0.1-ohm series resistance. As per the analysis, it can be concluded that with the rise in the series resistance value, there is a decrease in the maximum voltage and power value at a higher rate, whereas maximum current has significantly less effect of an increase in series resistance.

**E. EFFECT OF SHUNT RESISTANCE ( $R_{sh}$ )**

Light-generated current decreases with the decrease in shunt resistance. The shunt resistor causes a leakage current. Fig. 16 (a-c) shows the effect of shunt resistance on I-V and P-V

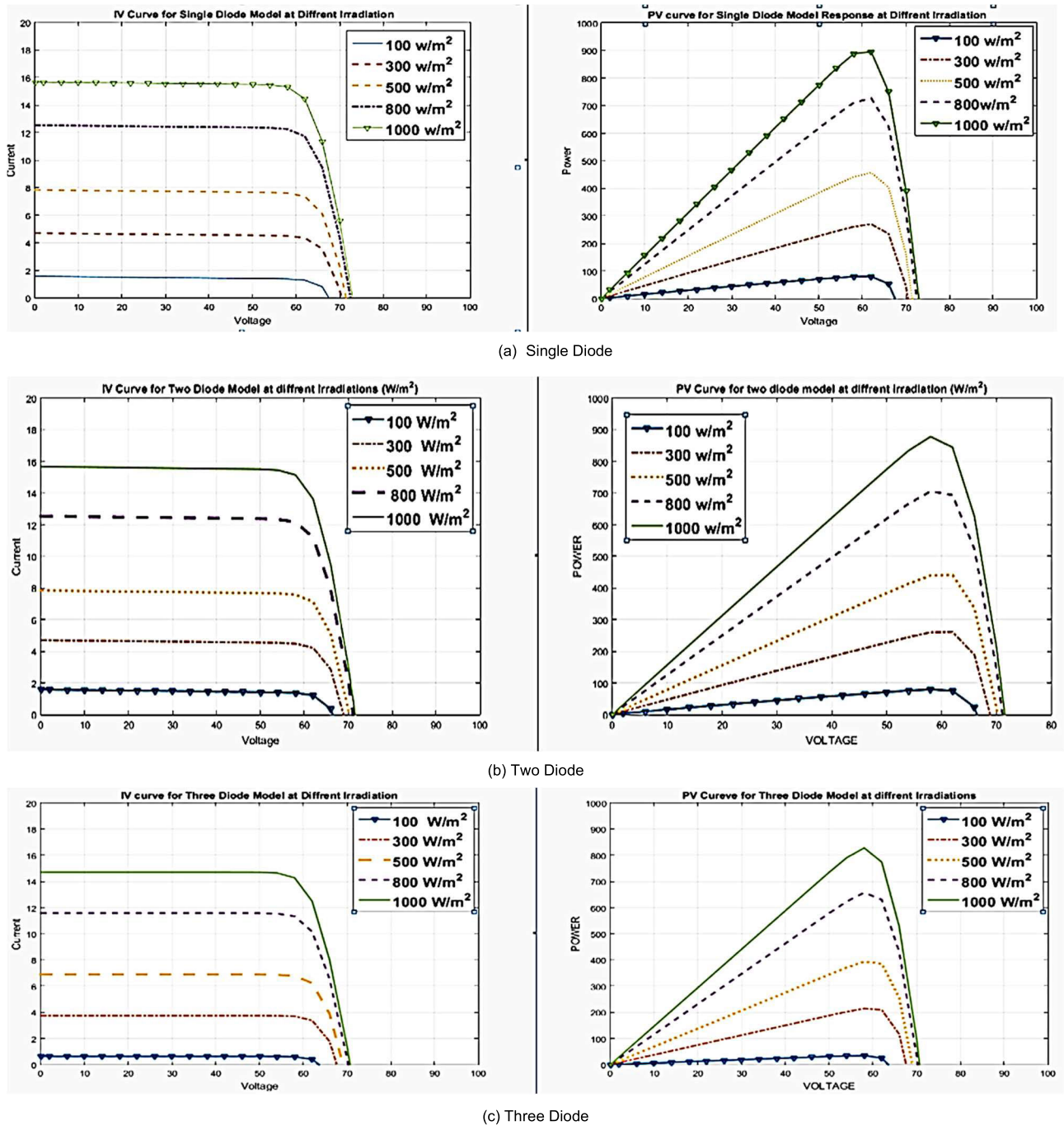


FIGURE 14. I-V and P-V characteristics of (a) single, (b) double, and (c) three diode model models at different Irradiation values.

curves at different shunt resistance values of 100, 200, 313.399, and 500 ohms. Table 9 shows the effective maximum value at different values of shunt resistance.

From Fig.16 and Table 9, it can be concluded that with the rise in the shunt resistance from 100-500 ohm, there is no change in the maximum voltage value. In contrast, maximum power and current values increase with the increase in the shunt resistance value. With the increase in the shunt resistance, there is an increase of 0.0725 watts/100 ohm

and negligible change in the maximum current value, i.e., 0.0048 amp/100 ohm. From the analysis, there is no effect of increasing the shunt resistance on the maximum voltage value, and negligible change can be found in the current value.

F. EFFECT OF SHADING

To determine the effect of shading, a PV model is created using the mathematical equations (1)-(12), expressed in

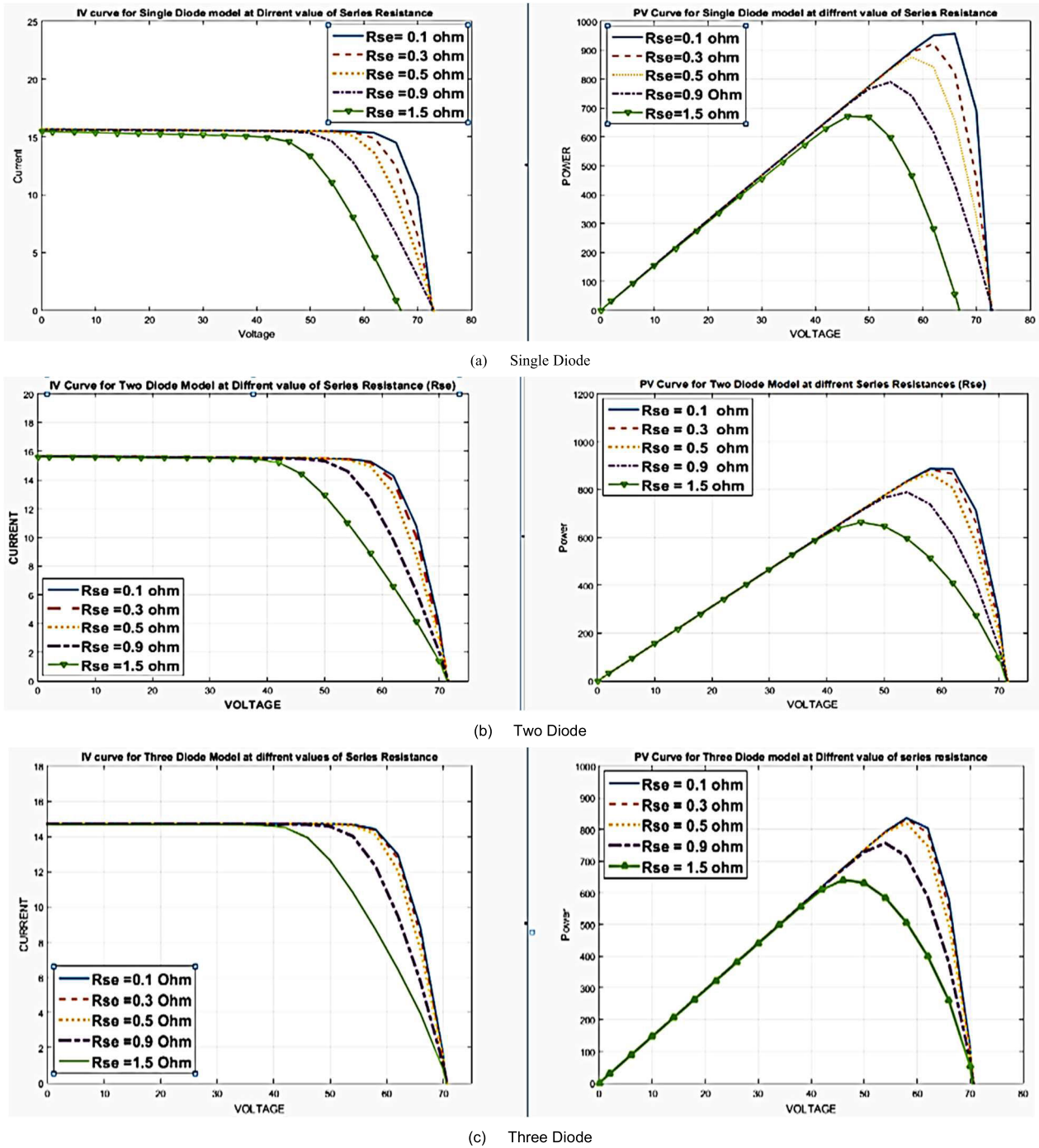


FIGURE 15. I-V and P-V curves of (a) single, (b) double, and (c) three diode models at different values of Series Resistance.

terms of five parameters for a single-diode model, two-diode model, and three-diode model. The concept is the same in all cases, but the diode equations are given in equations (8), (10), and (11), respectively. To analyse the effect of shading on the PV module, six irradiation is taken in a range of 200-1000 w/m<sup>2</sup> for 1-10 sec, and its effect is considered during that period. Table 10 represents the power and voltage obtained during the shading effect, and a single diode and

two diodes follow each other linearly for a few radiations. Still, the maximum power and voltage values differ in all three cases.

Fig. 17 and Fig. 18 represent the P-V and I-V curves during the shading effect for the designed model. It is seen from the results that even if a small portion suffers from the shading effect, the PV module fails to generate electricity. Due to the event of failure, the total power generation of the whole

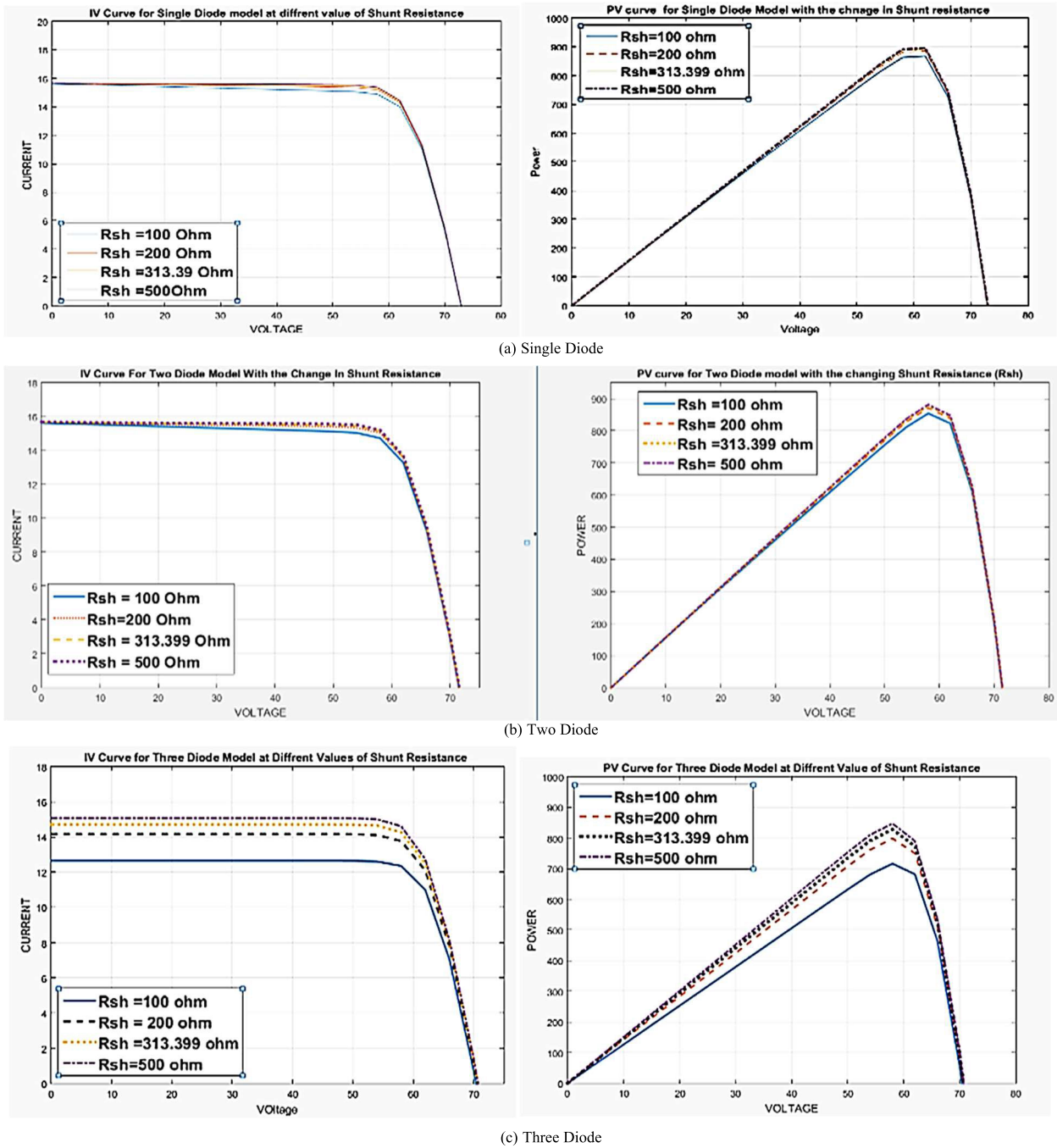


FIGURE 16. I-V curve and P-V curve for (a) Single, (b) Two (c) Three diode models for different values of Shunt Resistance.

PV array is reduced. From the result obtained, it can be said that the single diode model has a better P-V and I-V curve during the shading effect at 25°C temperature with  $V_{oc}$  value of 72 volts and  $I_{sc}$  of 15.48 amp, in comparison to the two and three diode model.

The three-diode model shows a better  $P_{max}$  at a lower temperature at 200w/m<sup>2</sup> than the single and two-diode models. With the decrease in the shading value (200-1000w/m<sup>2</sup>), the  $V_{max}$  and  $P_{max}$  value increases.  $P_{max}$  value

increase with 1.06 watt/w/m<sup>2</sup>, and  $V_{max}$  values increase with 0.0625 volts/w/m<sup>2</sup> for the single diode model. The increment in the maximum current value is 0.0121 amp/w/m<sup>2</sup>. Maximum voltage remains the same for single, two, and three-diode values at different shading conditions except at the lowest and highest value of shading conditions. From the analysis point of view, with the decrease in the shading effect, the maximum value of voltage, current, and power increases.

**TABLE 10.** Maximum power, voltage and current obtained during the shading effect.

Model	200 W/m <sup>2</sup> at t=2 sec			400 W/m <sup>2</sup> at t=5 sec			600 W/m <sup>2</sup> at t=7 sec			700 W/m <sup>2</sup> at t=9 sec			800 W/m <sup>2</sup> at t=10 sec			1000 W/m <sup>2</sup> at t >10 sec		
	$P_{max}$	$V_{max}$	$I_{max}$	$P_{max}$	$V_{max}$	$I_{max}$	$P_{max}$	$V_{max}$	$I_{max}$									
Single Diode	53.1	10	5.31	232	25	9.28	379	35	10.8	557	45	12.3	773	50	15.46	901.1	60	15.01
Two Diode	53.1	10	5.31	232	25	9.28	379	35	10.8	557	45	12.3	773	50	15.46	878	60	15.01
Three Diode	62.3	10	6.232	132.9	25	5.31	295.6	35	8.44	450	45	10	578	50	11.56	847.5	58	14.61

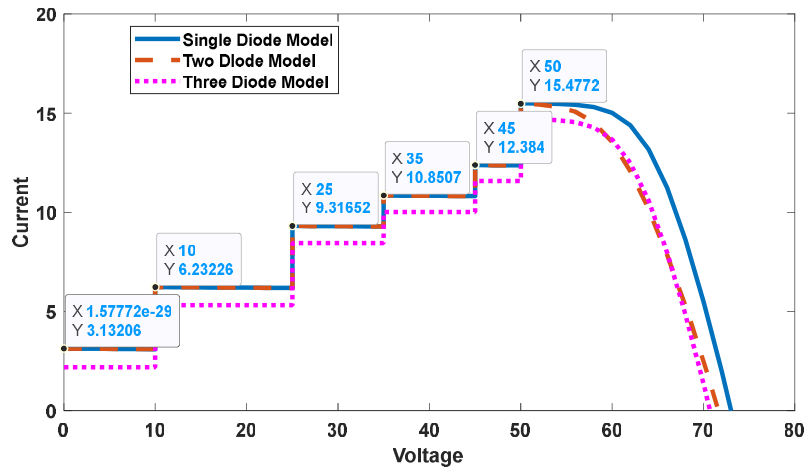


**FIGURE 17.** P-V characteristics for Single, Two, and Three Diode models during shading.

**TABLE 11.** Parameters of a single cell taken for different connection.

	Parameters (Single Cell)	Values (Single cell)
Short Circuit Current	$I_{sc}$	7.34
Open circuit Voltage	$V_{oc}$	0.6
Solar Irradiation	G	1000W/m <sup>2</sup>
Ideality Factor	H	1.5
Series Resistance	$R_{se}$	0.3938
Energy Gap	$E_{go}$	1.12
Steady Tolerance		1e <sup>-9</sup>
Number of Cells	$N_s$	36 (total)

**TABLE 12.**  $V_{oc}$ ,  $I_{sc}$ ,  $V_{max}$ ,  $I_{max}$ , and  $P_{max}$  corresponding to different connections (36 Cells).

Connections	$V_{oc}$ (Volts)	$I_{sc}$ (Amp.)	$V_{max}$ (Volts)	$I_{max}$ (Amp.)	$P_{max}$ (Watts)
Series	21.6	7.34	17.976	6.801	122.259
Parallel	0.6	264.2	0.5019	243.498	122.219
S-P	44.04	3.6	2.9916	40.8688	122.264
TCT	44.04	3.6	2.9845	40.9647	122.260
BL	44.04	3.6	3.0121	40.5750	122.216
HC	44.04	3.6	2.9825	40.99	122.257

**G. INTERCONNECTIONS OF CELLS TO FORM AN ARRAY**

Series, parallel, series-parallel, total cross-tied, bridge-linked, and honey-comb are the different types of connections used in PV modules. Different types of connection arrangements is shown in Fig. 4. These six different connections are compared to analyze their effect on maximum power. Table 11 gives the specification of a single cell, while Table 12 gives the  $V_{oc}$ ,  $I_{sc}$ ,  $V_{max}$ ,  $I_{max}$ , and  $P_{max}$  corresponding to different connections corresponding to different connections with 36 cells at STC. The series-parallel configuration is used to create the total cross-tied configuration. The honey-comb design has the benefits of total cross-tie and series-parallel configuration. The

I-V and P-V curve obtained for all the connections are given in Fig. 19(a) and Fig. 20 (a), where Fig. 19(b) and Fig. 20(b) are the magnified views of the curves. A small variation can be seen in  $V_{max}$  and  $I_{max}$ , maximum power ( $P_{max}$ ) for all the connections is somewhat equal at STC condition as given in Table 12. HC and BL connections have similar I-V performance as TCT, but the maximum power obtained in BL and HC is less.

The I-V curve for the BL connection has a smooth response but the P-V curve is not smooth. Total cross-tied connections are more accurate in terms of P-V and I-V curves when

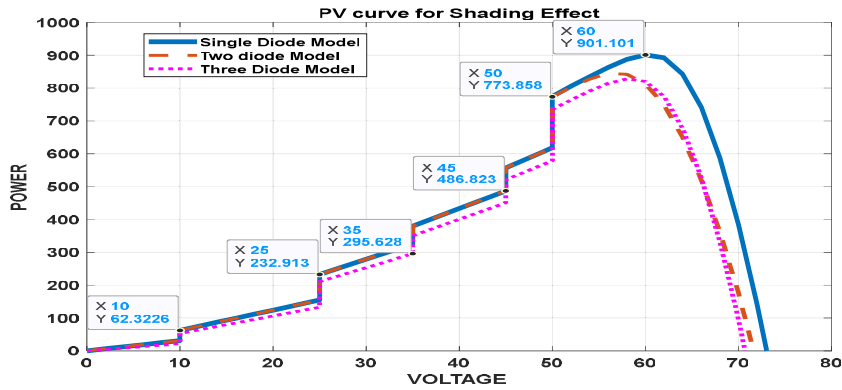
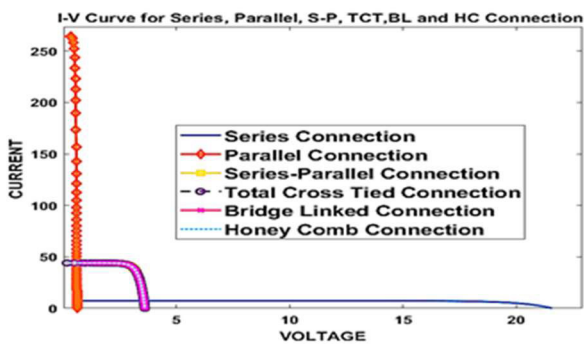
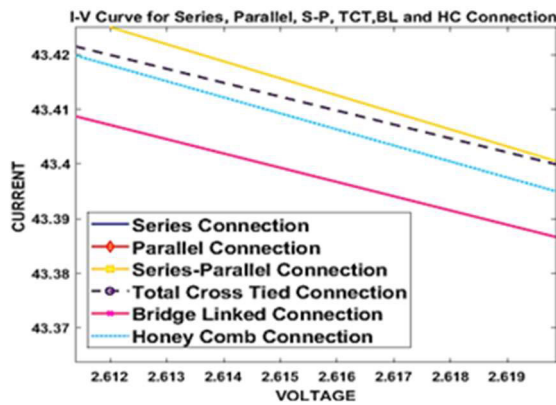


FIGURE 18. I-V characteristics for Single, Two, and Three diode models during shading.



(a) I-V curves



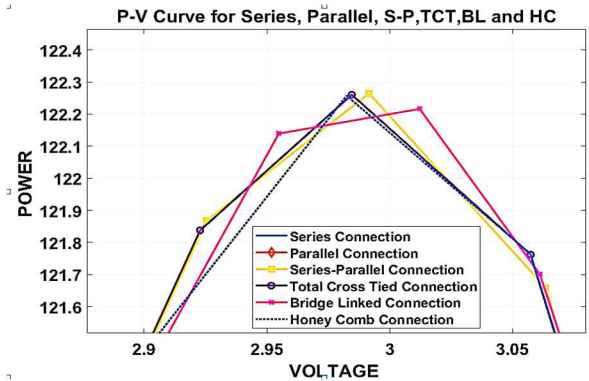
(b) Magnified view

FIGURE 19. (a) I-V curves for the different connections for single diode model (b) Magnified view of S-P, TCT, BL, and HC connection.

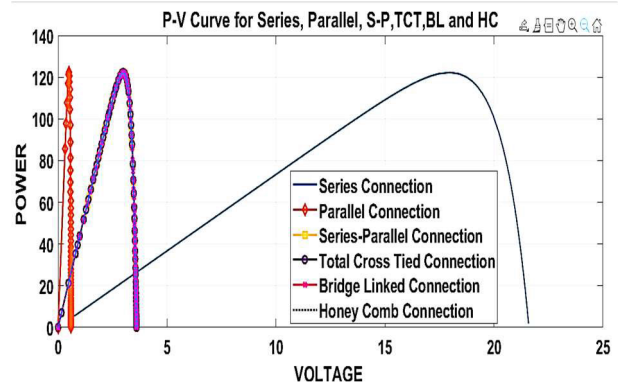
compared among series, parallel, series-parallel, and total crosstie connections.

### V. CONCLUSION

The mathematical Equation is utilized for single, two, and three-diode models in this research work to design a mathematical simulation model for different diode models, which is a replica of the original PV module, by using the corresponding I-V and P-V curves. After comparing the three models,



(a) P-V curve for the different connections



(b) Magnified view

FIGURE 20. (a) P-V curve for the different connections for single diode model (b) magnified view of S-P, TCT, BL, and HC connection.

at STC, it was concluded that the single-diode model had superior I-V and P-V curves with a maximum power output of 901.1 watts and maximum efficiency of 99.9%, whereas two and three-diode efficiency is 97.4% and 94.04%, but at lower temperatures, two and three-diode models perform better, and it was determined that with the increase in the number of diodes the  $P_{max}$  value decreases. The performance of the PV module is dependent on many factors like fill factor, material

effect, temperature coefficient, interconnections, degradation of PV module, variation in solar irradiation, module temperature, soiling, potential induced degradation, PV module tilt angle, parasitic resistance, and shading effect. Many of these parameters or factors affect the performance by affecting the voltage and current of the PV module and directly affect the overall performance and efficiency of the PV module/panel. In this paper, the effect of temperature, irradiation, shading, shunt resistance, series resistances, and different connections are analyzed for single, two, and three-diode models. The results demonstrate that:

- With the rise in “temperature” from 5°C to 50°C, the maximum voltage value decreases by 0.266 volt/°C, whereas the maximum current decreases by 0.0164 amp/°C (15.02-14.82 amp), and the maximum power value decreases by 4.044watts/°C (982-800 watts). The results demonstrate that at lower temperatures, the current remains almost constant, but as the temperature rises, the current value changes somewhat, but the large variation can be in the voltage value, which indirectly decreases the maximum power. A single diode has a better response than two and three-diode models.
- With the rise in irradiation from 100-1000w/m<sup>2</sup>, there is an increase in the Maximum power value of 80.04 watt/100w/m<sup>2</sup> and the current value increases at 0.1367 amp/100 w/m<sup>2</sup> value, and very less change takes place in the maximum voltage value, i.e., 0.02 volts/100w/m<sup>2</sup> with the increase in irradiation value. The results show that PV current has a greater influence when irradiation increases and decreases than the voltage. A single diode has a better response than two and three-diode models.
- With the increase in the “series resistance” value from 0.1 to 1.5 ohm, the value of maximum voltage decreases by 12.85714 volt/0.1 for a single diode, and maximum power decreases with the increase in the series resistance by a value of 216.785 watts/0.1-ohm and the maximum current value keep increasing to a certain value and then start decreasing after 0.5 ohms, overall, very negligible change is found in the current value. Whereas with the increase in “shunt resistance” from 100-500ohm, there is no change in the maximum voltage value, but maximum power increase with 0.0725 watts/100 ohm, and there is negligible change in the maximum current value, i.e. 0.0048 amp/100 ohm. A single diode has a better response than two and three-diode models. Both voltage and current levels are affected by  $R_{se}$ , the current value is mainly influenced due to changes in series resistance, and the output power increases as  $R_{sh}$  increases.
- With the decrease in the “shading” value (200-1000w/m<sup>2</sup>), the  $P_{max}$  value increases by 1.06 watt/w/m<sup>2</sup> and  $V_{max}$  values increase with 0.0625 volts/watt/m<sup>2</sup> for the single diode model, and the maximum current value

increases with 0.0121 amp/watt/m<sup>2</sup>. The maximum voltage remains the same for single, two, and three-diode values at different shading conditions except at the lowest and the highest value of a shading condition. A single diode has a better response than two and three-diode models.

- It is observed that for the single-diode model, the TCT connection is more accurate in terms of P-V and I-V curves than series, parallel, and SP. HC and BL connections have similar I-V performance as that of TCT, but the maximum power obtained in BL and HC is less.

The submitted research explained the impact of parameter variations on the I-V and P-V curves of a designed solar PV module/panel for 901.2 watts. If a DC-DC converter is utilized at the model’s output, the power of the cell can be increased, and smooth curves for various environmental conditions can be obtained. An MPPT controller may be used to track the maximum power from the panels under various climatic situations. This includes as well as the global maximum power point of the panel under partial shading conditions. Experimentally, we can evaluate the impact of irradiance, temperature, soiling, material, cooling, Module tilt angle, and degradation of PV module to the extent that a correlation between hotspots and different connection topologies can be discovered.

#### AUTHOR CONTRIBUTIONS

All authors have contributed to the completion of research work and agreed to the published version of the manuscript.

#### ACKNOWLEDGMENT

The authors are thankful to the management of Gautam Buddha University, India, for extending the support of this research work.

#### CONFLICTS OF INTEREST

The authors declare no conflict of interest.

#### REFERENCES

- [1] D. Yadav, N. Singh, and V. S. Bhadoria, “Comparison of MPPT algorithms in stand-alone photovoltaic (PV) system on resistive load,” in *Machine Intelligence and Smart Systems (Algorithms for Intelligent Systems)*. Singapore: Springer, 2021, pp. 385–400.
- [2] D. Yadav and N. Singh, “Comparative analysis of conventional, artificial intelligence, and hybrid-based MPPT technique for 852.6-watt PV system,” *Int. J. Social Ecol. Sustain. Develop.*, vol. 13, no. 2, pp. 1–23, Jun. 2022, doi: 10.4018/ijesed.302463.
- [3] D. Agarwal, K. Verma, and S. Urooj, *Energy Harvesting: Enabling IoT Transformations*. Boca Raton, FL, USA: Chapman & Hall, 2022.
- [4] G. Fotis, C. Dikeakos, E. Zafeiropoulos, S. Pappas, and V. Vita, “Scalability and replicability for smart grid innovation projects and the improvement of renewable energy sources exploitation: The FLEXI-TRANSTORE case,” *Energies*, vol. 15, no. 13, p. 4519, Jun. 2022, doi: 10.3390/en15134519.
- [5] S. Sambhi, H. Sharma, V. Bhadoria, P. Kumar, R. Chaurasia, G. Fotis, and V. Vita, “Technical and economic analysis of solar PV/diesel generator smart hybrid power plant using different battery storage technologies for SRM IST, Delhi-NCR campus,” *Sustainability*, vol. 15, no. 4, p. 3666, Feb. 2023, doi: 10.3390/su15043666.

- [6] T. T. Yetayew and T. R. Jyothsna, "Improved single-diode modeling approach for photovoltaic modules using data sheet," in *Proc. Annu. IEEE India Conf. (INDICON)*, Dec. 2013, pp. 1–6.
- [7] S. Bader, X. Ma, and B. Oelmann, "A comparison of one- and two-diode model parameters at indoor illumination levels," *IEEE Access*, vol. 8, pp. 172057–172064, 2020, doi: 10.1109/access.2020.3025146.
- [8] A. Kumar and R. Agarwal, "Mathematical modeling and analysis of single-diode, double-diode and triple diode based PV module," in *Proc. Int. Conf. Advancement Technol. (ICONAT)*, Jan. 2023, pp. 1–6.
- [9] I. Ali, S. Kumar, and S. Siddiqui, "Performance analysis of different solar models based on the solar cell parameters," *Indian J. Pure Appl. Phys.*, vol. 59, no. 3, pp. 263–270, 2021.
- [10] A. M. Humada, S. Y. Darweesh, K. G. Mohammed, M. Kamil, S. F. Mohammed, N. K. Kasim, T. A. Tahseen, O. I. Awad, and S. Mekhilef, "Modeling of PV system and parameter extraction based on experimental data: Review and investigation," *Sol. Energy*, vol. 199, pp. 742–760, Mar. 2020.
- [11] D. Yadav, N. S. Pal, and M. A. Ansari, "Analyzing the effects of coal and dust on solar panel and improving the fill factor by using spray cooling," *Recent Trends Electron. Commun. Syst.*, 2019.
- [12] S. Djordjevic, L. Pantic, M. Krstic, I. Radonjic, M. Mancic, and A. Pantic, "Enhancing monocrystalline solar module efficiency through front-surface cooling with 96% alcohol," *Appl. Sci.*, vol. 13, no. 9, p. 5331, Apr. 2023, doi: 10.3390/app13095331.
- [13] T. Dewi, P. Risma, and Y. Oktarina, "A review of factors affecting the efficiency and output of a PV system applied in tropical climate," *IOP Conf. Ser., Earth Environ. Sci.*, vol. 258, May 2019, Art. no. 012039, doi: 10.1088/1755-1315/258/1/012039.
- [14] K. V. Vidyandanand, "An overview of factors affecting the performance of solar PV systems," *Energy Scan, House J. Corporate Planning, NTPC Ltd.*, vol. 27, pp. 2–8, Feb. 2017.
- [15] D. T. Cotfas, P. A. Cotfas, and O. M. Machidon, "Study of temperature coefficients for parameters of photovoltaic cells," *Int. J. Photoenergy*, vol. 2018, pp. 1–12, Apr. 2018, doi: 10.1155/2018/5945602.
- [16] R. Ramaprabha and B. L. Mathur, "A comprehensive review and analysis of solar photovoltaic array configurations under partial shaded conditions," *Int. J. Photoenergy*, vol. 2012, pp. 1–16, Mar. 2012, doi: 10.1155/2012/120214.
- [17] Y.-J. Wang and P.-C. Hsu, "An investigation on partial shading of PV modules with different connection configurations of PV cells," *Energy*, vol. 36, no. 5, pp. 3069–3078, 2011, doi: 10.1016/j.energy.2011.02.052.
- [18] F. Belhachat and C. Larbes, "PV array reconfiguration techniques for maximum power optimization under partial shading conditions: A review," *Sol. Energy*, vol. 230, pp. 558–582, Dec. 2021, doi: 10.1016/j.solener.2021.09.089.
- [19] M. S. Honnurvali, N. Gupta, K. Goh, and T. Umar, "Measurement, modeling and simulation of photovoltaic degradation rates," in *Modelling, Simulation and Intelligent Computing* (Lecture Notes in Electrical Engineering). Singapore: Springer, 2020, pp. 56–63.
- [20] F. Shaik, S. S. Lingala, and P. Veeraboina, "Effect of various parameters on the performance of solar PV power plant: A review and the experimental study," *Sustain. Energy Res.*, vol. 10, no. 1, pp. 1–23, Apr. 2023, doi: 10.1186/s40807-023-00076-x.
- [21] D. Yadav and N. Singh, "Application of artificial neural network in maximum power point tracking for different radiation, temperature," in *Proc. Int. Conf. Sci. Natural Comput.* Singapore: Springer, 2021, pp. 73–87.
- [22] M. Kermadi, V. J. Chin, S. Mekhilef, and Z. Salam, "A fast and accurate generalized analytical approach for PV arrays modeling under partial shading conditions," *Sol. Energy*, vol. 208, pp. 753–765, Sep. 2020, doi: 10.1016/j.solener.2020.07.077.
- [23] A. Machniewics, D. Korea, and D. Heim, "Effect of transition temperature on the efficiency of PV/PCM," in *Proc. 6th Int. Building Phys. Conf. (IBPC)*, vol. 78, 2015, pp. 1684–1689.
- [24] S. Pingel, O. Frank, M. Winkler, S. Daryan, T. Geipel, H. Hoehne, and J. Berghold, "Potential induced degradation of solar cells and panels," in *Proc. 35th IEEE Photovolt. Spec. Conf.*, Jun. 2010, pp. 2817–2822.
- [25] S. Şevik, A. Koçer, H. Ince, and F. E. Tombus, "Determination of optimum tilt angle of the solar collector and evaluation of the position of the existing buildings in terms of solar potential," *Archit. Eng. Des. Manag.*, vol. 18, no. 6, pp. 812–828, 2022.



**DILIP YADAV** received the B.Tech. degree in electronics and engineering from the Moradabad Institute of Technology, Moradabad, Uttar Pradesh, and the M.Tech. degree in power systems from Gautam Buddha University, Greater Noida, in 2014, where he is currently pursuing the Ph.D. degree in electrical engineering. He has published more than 24 research papers, including book chapters, articles, and international conference papers. His research interests include renewable energy power generation, maximum power tracking, artificial intelligence, optimization techniques, and converters.



**NIDHI SINGH** is currently with the Department of Electrical Engineering, Gautam Buddha University, Greater Noida, as the Head of the Department. She did research in control engineering. Her skills and expertise are in MATLAB simulation, controller design, control engineering, distributed systems, control projects, control theory, and renewable energy. Her research interests include model order reduction of large-scale dynamic systems, applications of soft computing techniques in various control problems, and energy harvesting using photovoltaic systems.



**VIKAS SINGH BHADORIA** received the B.E. and M.E. degrees in electrical and electronics engineering from RGPV, Bhopal, India, in 2005 and 2009, respectively, and the Ph.D. degree in power systems from Gautam Buddha University, Greater Noida, Uttar Pradesh, India, in 2018. He is currently the Deputy Training and Placement Officer with Shri Vishwakarma Skill University, Palwal, Haryana. His research interests include power system planning, power system reliability, and power system restructuring.



**VASILIKI VITA** received the B.E. degree in electrical engineering from the Higher School of Pedagogical and Technical Education (ASETEM/SELETE), Greece, in 2000, the first M.Sc. degree in control systems from The University of Sheffield, U.K., in 2002, the second M.Sc. degree in fundamental and applied cognitive science from the National and Kapodistrian University of Athens, Greece, in 2015, and the Ph.D. degree in electrical engineering from the City, University of London, U.K., in 2016. She is the author of more than 90 papers in international journals and conferences. Her research interests include transmission and distribution grids, distributed generation, optimization, lightning performance, electric vehicles, and artificial intelligence.



**GEORGIOS FOTIS** received the Diploma and Ph.D. degrees in electrical engineering from the National Technical University of Athens (NTUA), in 2001 and 2006, respectively. From 2006 to 2008, he was a Research Assistant with the NTUA's High Voltage Laboratory and a Lecturer (fixed term), teaching high voltages. He has been a Independent Power Transmission Operator (I.P.T.O.) with the Transmission System Operation and Control Department, since 2009.

Also, he has been an Assistant Professor (fixed term), teaching electric power systems and high voltages with the Department of Electrical and Electronics Engineering Educators, School of Pedagogical and Technological Education (ASPETE), since 2010. He is the author of one book and more than 70 papers in international journals and conferences. His research interests include power systems, transmission and distribution grids, high voltages, electromagnetic compatibility, and electrostatic discharge.



**THEODOROS I. MARIS** received the Diploma and Ph.D. degrees in electrical engineering from the School of Engineering, University of Patras, Greece, in 1984 and 1994, respectively. He is a Professor with the Control Systems and Industrial Automation Laboratory, National and Kapodistrian University of Athens. His research interests include electric energy systems, direct current interconnections, high voltage direct current converters, electrical drives, photovoltaic inverters, transmission and distribution lines, and artificial neural networks.

• • •



**ELEFThERIOS G. TSAMPASIS** received the B.E. degree in electrical engineering from the Technological Education Institute of Chalkis, Greece, in 1997, the M.Sc. degree in electronics from the University of Hertfordshire, U.K., in 1998, and the Ph.D. degree from the Department of Computer Engineering and Informatics, University of Patras. He is a Lecturer with the Control Systems and Industrial Automation Laboratory, National and Kapodistrian University of Athens. His research

interests include automations systems, transmission and distribution grids, distributed generation, optimization, electric vehicles, artificial intelligence, electric energy systems, photovoltaic inverters, and artificial neural networks.